

Quantifying the Electrocatalytic Turnover of Single Soft Nanoparticles: Vitamin B₁₂ Mediated Dehalogenation

W. Cheng and R. G. Compton*

Department of Chemistry, Physical & Theoretical Chemistry Laboratory, Oxford University, South Parks Road, Oxford, OX1 3QZ, United Kingdom, Fax: (+44) 1865-275-410

*Corresponding email: richard.compton@chem.ox.ac.uk

Abstract:

We report the electrocatalytic dehalogenation of trichloroethylene by single soft nanoparticles of VB₁₂ containing droplets, and find that the binding between Co (I), the reduced form of Co (III), and TCE is likely a chemically reversible process and in particular using this model system quantify the turnover number and the kinetics of catalytic reactions at individual single soft nanoparticles in real time.

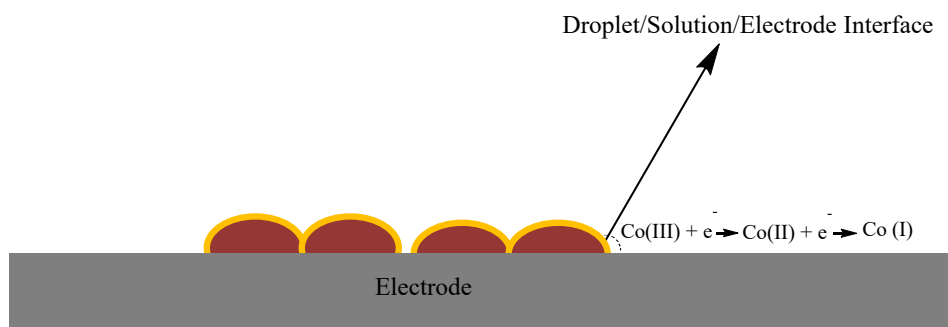
Measuring the catalytic kinetics of individual nanoparticles is challenging because the charge transfer can only be crudely estimated when using an ensemble^[1]. Rather single nanoparticles measurements are essential. The electrocatalytic reaction at the surface of single metal nanoparticles can be observed when such nanoparticles collide with an inert electrode that otherwise could not electrocatalyse the reaction as a result of their random collision as a consequence of their Brownian motion, so called “nano impacts”^[2]. Most recently nano impacts has extended to characterise single soft nanoparticles^[3] such as liposomes^[3a], vesicles^{[3b],[3k]}, cytomegalovirus^[3c], micelles^[3d], droplets and its mediated oxygen reduction^[3e-i], and macromolecules^[3j]. The electron transfer is revealed by probing redox molecules or catalysts encapsulated inside soft nanoparticles in contrast to the mediated charge transfer takes place at the surface of metal nanoparticles. To date, there are few reports on reactions catalysed by soft nanoparticles compared to the extensive studies of metal nanocatalysts^[4]. Most particularly, the kinetics and single turn-over efficiency of soft nanoparticles of any types have never been quantified at single-individual-nanoparticle resolution.

As a natural redox enzyme, electron transfer through Co (III), the redox centre in Vitamin B₁₂ has found diverse uses in synthesis, bioremediation and biocatalysis^[5]. There has been significant interests in electrocatalytic reactions by Vitamin B₁₂^[6]. In particular, the reductive dehalogenation of trichloroethylene (TCE) through Co (III) was examined^[6a, 6d] and recently has suggested to occur via

the intermediary of halogen-cobalt bond formation^[7]. In this paper using Vitamin B₁₂ as a model system, we report the electrocatalytic dehalogenation of trichloroethylene by single soft nanoparticles (nano-droplet) which contain Vitamin B₁₂ dissolved in water/glycerol encapsulated by emulsifiers. We find that the binding between Co (I), the reduced form of Co (III), and TCE is likely a chemically reversible process and in particular quantify the catalytic efficiency, interrogating soft nanoparticle catalysis at the single-nanoparticle level in real time with single-turnover resolution. To our knowledge, this is the first report to *quantitatively* measure the turnover number and the kinetics of catalytic reactions at individual soft nanoparticles.

The ensemble electrochemical behaviour of VB₁₂ emulsions was first investigated by dropcasting emulsions of droplets to form an ensemble on a macro glassy carbon (GC) electrode (diameter = 3 mm) and recording cyclic voltammograms. Figure S1(a) shows the cyclic voltammograms for a glassy carbon macroelectrode modified with 2 μ L VB₁₂ droplets immersed in phosphate buffered saline (PBS) buffer (pH = 6.8) at different scans between 20 mV/s to 400 mV/s. Two reduction peaks were observed around -0.10 V and -0.95 V versus the saturated calomel reference electrode (SCE), likely corresponding to the two stages of one-electron transfer $\text{Co(III)} + e^- \longrightarrow \text{Co(II)}$ and $\text{Co(II)} + e^- \longrightarrow \text{Co(I)}$, respectively ^[8].

The peak current show a linear dependence on scan rates (Figure S1(b)), indicating a surface controlled process, while the integrated charge under the first reductive peak amounts to less than 2% of the total theoretical charge if assuming the immobilised VB₁₂ droplets are completely reduced from Co (III) to Co (II) and knowing the mass of materials dropcasted (see SI). It was inferred that the charge injection occurred at the three phase boundary formed between the surface immobilised droplets, the electrode and the solution ^[9] (Scheme 1).



Scheme 1: Reduction of Vitamin B-12 droplets dropcast on a macro electrode

Voltammetric methods were further used to study the electrocatalytic behaviour of immobilised VB₁₂ droplet in the presence of TCE, as shown in Figure 1. It was found that additions of TCE caused large increases in the second cathodic current for electron transfer between Co (II) and Co (I) at -1.1 V, which are due to the catalytic reduction of TCE. Comparing the voltammograms without TCE (blue line) or without VB₁₂ (black line) clearly demonstrates the electrocatalytic activity of VB₁₂ droplets modified on the electrode for the reduction of trichloroethylene Co(III) + 2e⁻ → Co(I), followed by the reduction of TCE through Co(I), Co(I) + trichloroethylene (TCE) $\xrightarrow{+H^+, -Cl^-}$ Co(III) + dichloroethylene (DCE) [6d].

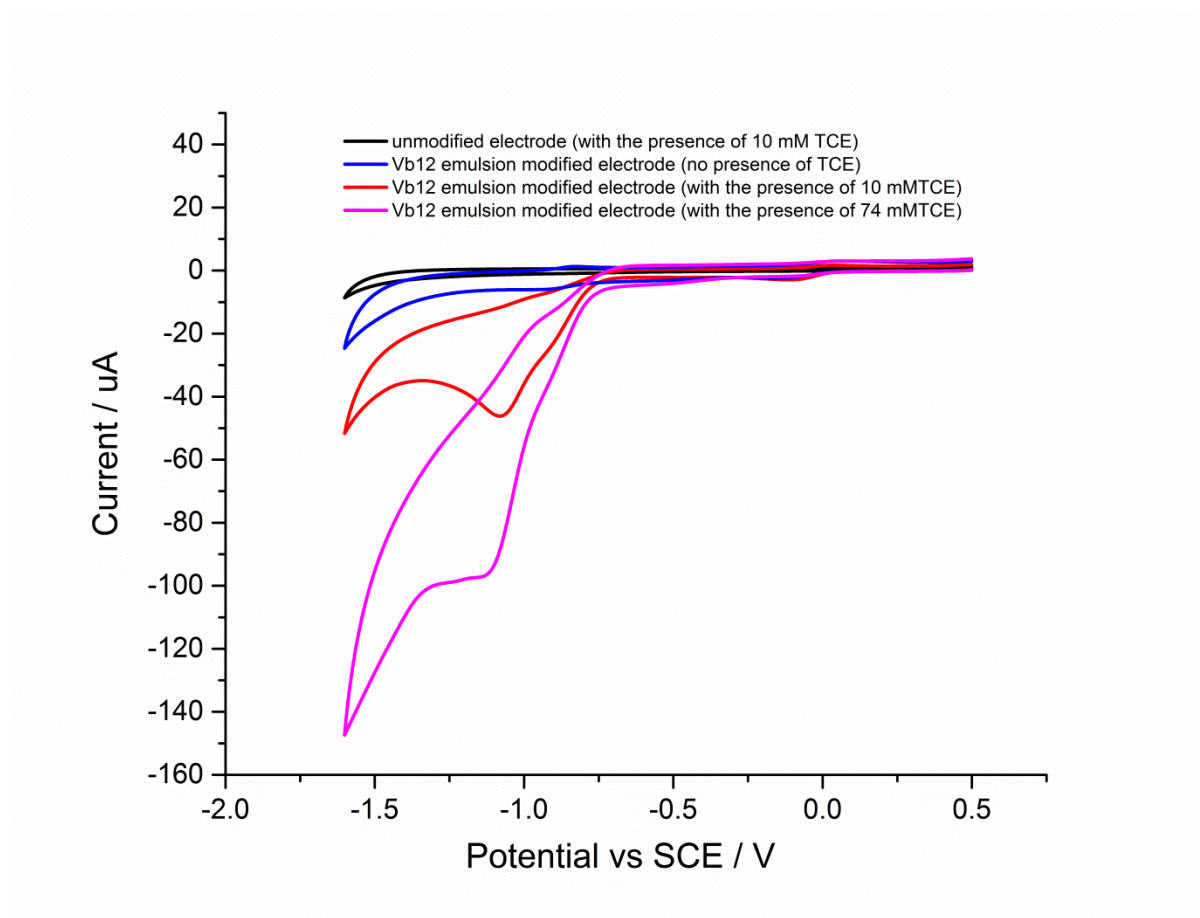


Figure 1 Voltammograms of glassy carbon electrode modified with VB₁₂ droplets at 200 mV/s in 100 mM PBS buffer (pH 6.8) containing 74 mM TCE (magenta line), 10 mM TCE (red line), 0 mM TCE (blue line) and voltammogram of bare glassy carbon electrode in PBS buffer containing 10 mM TCE (pH 6.9) (black line).

Whilst the voltammetry shown in Figure 1 and S1, S2 indicates catalysis of the reduction of TCE by the Co (III) oxidative state of VB₁₂, because of the uncertain geometry of the droplet modified electrode and the imprecise nature of the three phase boundary it is hard, if not impossible to extract quantitative information. We therefore turn to nano-impacts to clarify and quantify the kinetics and mechanism.

Next, a carbon microelectrode was immersed in PBS buffer solution and known amounts of dispersed VB₁₂ droplets and trichloroethylene added. In the absence of TCE, clear reductive (Faradaic) current spikes were detected at sufficient negative potentials more negative than -0.3 V (Figure 2(a)). A “voltammogram” of direct electrochemical reduction of single VB₁₂ droplet was obtained by recording the average charge (the number of recorded impact events for each potential was greater than 100) transferred as a result of direct Faradaic reduction of VB₁₂ droplets versus different potentials (Figure 2(b)). The onset of spikes were found to be dependent on the reduction potential and no reductive spikes of VB₁₂ droplet at the reductive potentials of +0.1 V or more positive, suggesting the spikes correspond to Faradaic reduction of VB₁₂ containing droplets. The presence of two plateaus in this “voltammogram” suggest two steps of reduction of single droplets containing VB₁₂, respectively resulted from reduction of Co (III) to Co (II), and subsequent reduction of Co (II) to Co (I) upon a single droplet impacting at higher potential. The average charge value at second plateau is almost twice of that at the first plateau, consistent with double-electron transfer occurring upon a single nanoparticle impacts at very negative potentials.

Analogous nano-impact experiments of single VB₁₂ droplets were conducted in PBS buffer containing 16 mM TCE. At lower potential (up to -0.5 V), the amplitudes of spikes are similar to those found without TCE, while the amplitude of the spikes significantly increased when the potential increased to -0.75 V or more negative (Figure 2), indicating at a sufficient high potential TCE starts to be involved in the charge transfer and is reduced when single VB₁₂ droplets collide with the electrode.

To further investigate the catalytic reduction of TCE by single VB₁₂ droplets, the average charge of individual spikes at a range of potentials was calculated and then was plotted as a function of potential, as illustrated in Figure 2b. Comparing this catalytic “voltammogram” of single VB₁₂ droplets (red dots) to the “voltammogram” of direct reduction of single VB₁₂ droplets (black squares), the value of average charge of individual spikes is found significantly larger at potentials above -0.75 V suggesting that catalytic reduction of TCE accompanies the direct reduction of single nanodroplets and contributes to the charge injection when individual VB₁₂ nanodroplet collide with the electrode, while the average charge of individual spikes is similar at potentials below -0.5 V, indicating that the catalytic reduction of TCE can only accompany the electron transfer between Co (II) to Co (I) under sufficient higher potential, and the active “catalyst” is the reduced form Co (I) [6a, 6d].

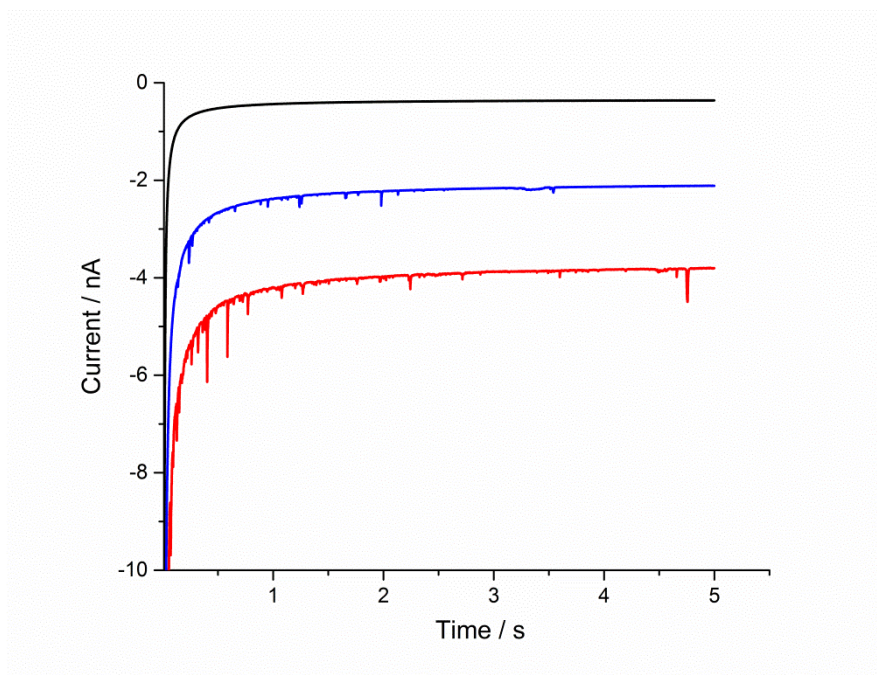


Figure 2(a)

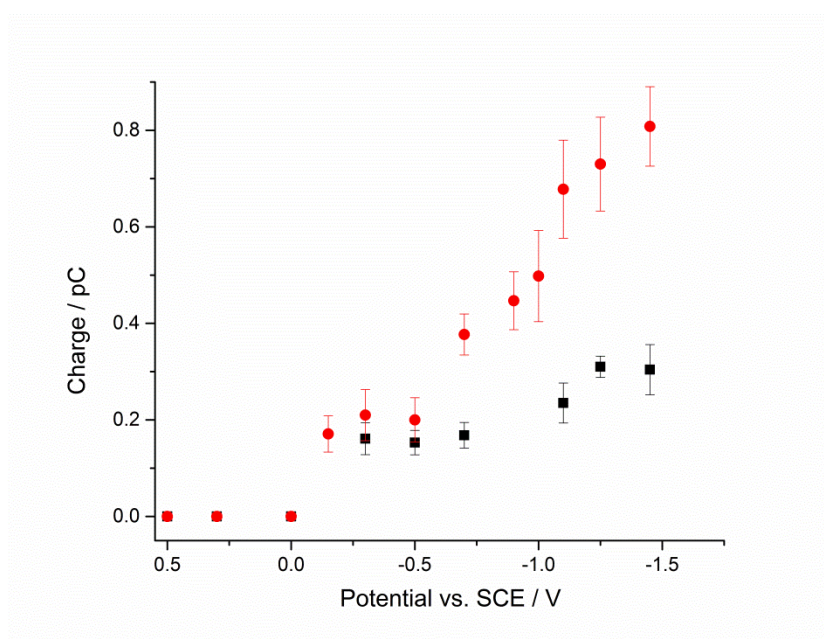


Figure 2(b)

Figure 2(a) Representative chronoamperometric profiles of nano-impacts at -1.25 V versus SCE. in PBS buffer (100 mM; pH 6.9) containing: 16 mM TCE only (black); VB₁₂ nanodroplets only (blue); VB₁₂ nanodroplets and 16 mM TCE (red); (b) “voltammograms” of single soft nanoparticles: VB₁₂ nanodroplets only (black squares), VB₁₂ nanodroplets and 16 mM TCE (red dots).

Subsequently, to obtain kinetic information of the reduction of TCE catalysed by the single soft nanoparticles of VB₁₂ containing droplets, “catalytic voltammograms” were obtained under different added concentrations of TCE (Figure 3). The amplitudes of spikes at certain high potentials generally increased with increased concentrations of TCE, further confirming that the spikes observed at higher potentials correspond to catalytic reduction of TCE through single VB₁₂ nanodroplets impacting the electrode. The distribution of the charge from electrocatalytic reduction by individual soft nanoparticles indicates the nanoparticle-dependent heterogeneity for single soft nanoparticles (Figure S4).

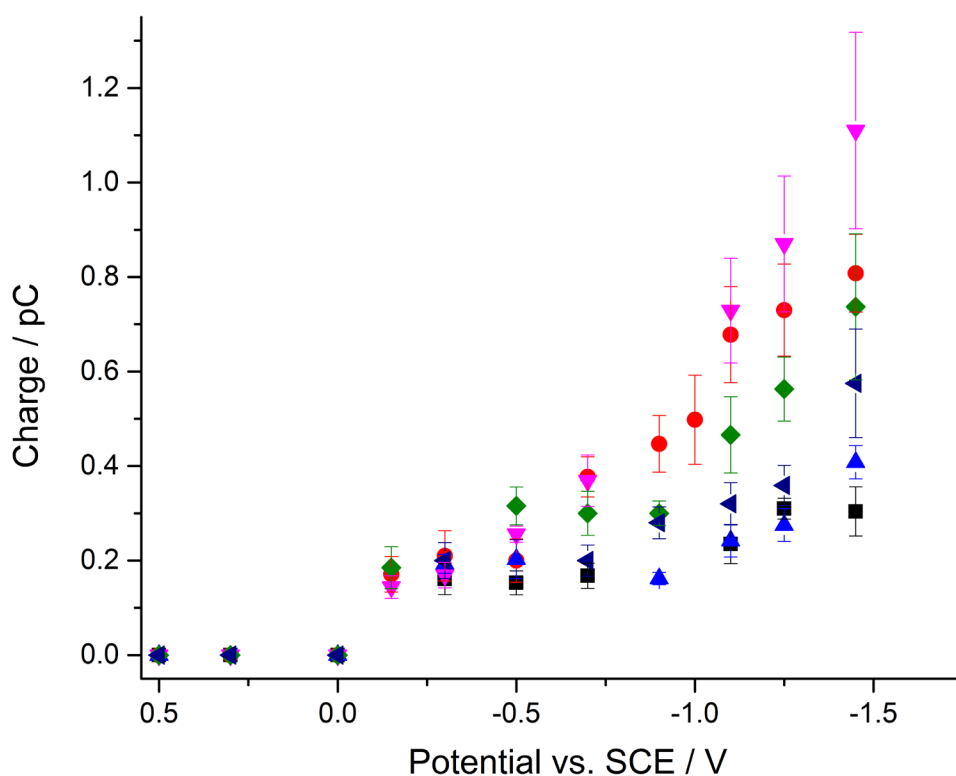
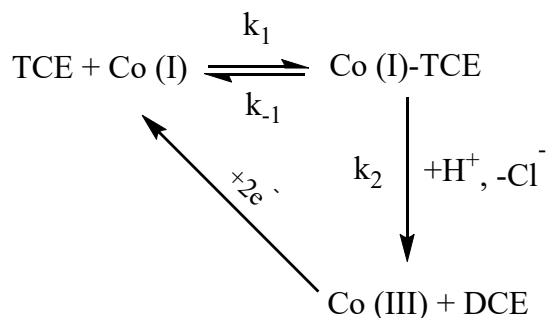


Figure 3 Catalytic “voltammograms” of single soft nanoparticles at various substrate concentrations: Average charge Q for single VB₁₂ droplets impacts vs. potential E in PBS buffer with increasing TCE concentrations: 0 mM (black), 5 mM (blue), 7.4 mM (navy), 9.5 mM (green), 16 mM (red), and 74 mM (magenta).



Scheme 2: Electrocatalytic reductive dehalogenation of TCE by VB₁₂

To quantify the catalytic efficiency of dehalogenation by single nanodroplet, we term the effective turn-over number (k_{eff}) at different concentrations of TCE substrates for electrocatalytic dehalogenation at single VB₁₂ soft nanoparticle by Equation 1:

$$k_{eff} = \frac{m}{t \cdot m_{cat}} = \frac{(Q_{total} - Q_1)}{t \cdot Q_1}$$

Equation 1

where m is the moles of TCE catalytically reduced or dichloroethylene (DCE) catalytically produced, m_{cat} is the moles of catalyst, which in this case are moles of VB₁₂ in single nano-droplet. m_{cat} can be estimated as $\frac{AQ_1}{2F}$, where F is the Faraday constant, A is the Avogadro constant, Q_1 is charge transferred for the reduction of single VB₁₂ nanodroplet corresponding to reduction of Co (III) to Co (I). t is the duration of the impact times. m can be thus derived from the total charge (Q_{total}) transferred for dehalogenation of trichloroethylene by single VB₁₂ nanodroplets, and the charge transferred (Q_1) between Co (III) to Co (I) before the dehalogenation is initiated, as $\frac{A(Q_{total}-Q_1)}{2F}$. Two moles electrons were transferred for catalytic dehalogenation from one mole TCE to DCE (Scheme 2) [6].

k_{eff} can be estimated using impact times t from nano-impacts experiments (see SI) to be $84 \pm 11 \text{ s}^{-1}$, $133 \pm 27 \text{ s}^{-1}$, $192 \pm 40 \text{ s}^{-1}$, $203 \pm 21 \text{ s}^{-1}$, $327 \pm 61 \text{ s}^{-1}$ for various concentrations of TCE substrates from 5 mM up to 74 mM. Further, the effective turn-over number (k_{eff}) at different concentrations of TCE substrates was plotted against the TCE concentration. Interestingly, a Michaelis-Menten like response was observed, as shown in Figure S6, indicating a probably reversible binding between Co (I) and TCE (Scheme 2). If this is the case, when the concentration of TCE reaches higher, at which all the reduced Co (I) form of VB₁₂ in single nanodroplet is actively bound, increasing TCE substrate will not increase the rate of the reaction, known as the maximum turn-over number k_2 or k_{cat} .

To verify the hypothesis and quantify the catalytic kinetics, the reaction rate of electrocatalytic dehalogenation is expressed as (see SI):

$$\frac{d[DCE]}{dt} = \frac{k_2 [TCE][Co(I)]_{total}}{K + [TCE]}$$

Equation 2

$$\text{thus } k_{eff} = \frac{k_{cat} [TCE]}{K + [TCE]}$$

Equation 3

$$\text{then } \frac{1}{K_{eff}} = \frac{1}{k_{cat}} + \frac{K}{k_{cat}} \frac{1}{[TCE]}$$

Equation 4

where K is the kinetic constant $\frac{(k_{-1}+k_2)}{k_1}$ (See SI), $[TCE]$ is the trichloroethylene concentration; $[DCE]$ is the dichloroethylene concentration; $[Co(I)]_{total}$ is the *total* Co (I) concentration.

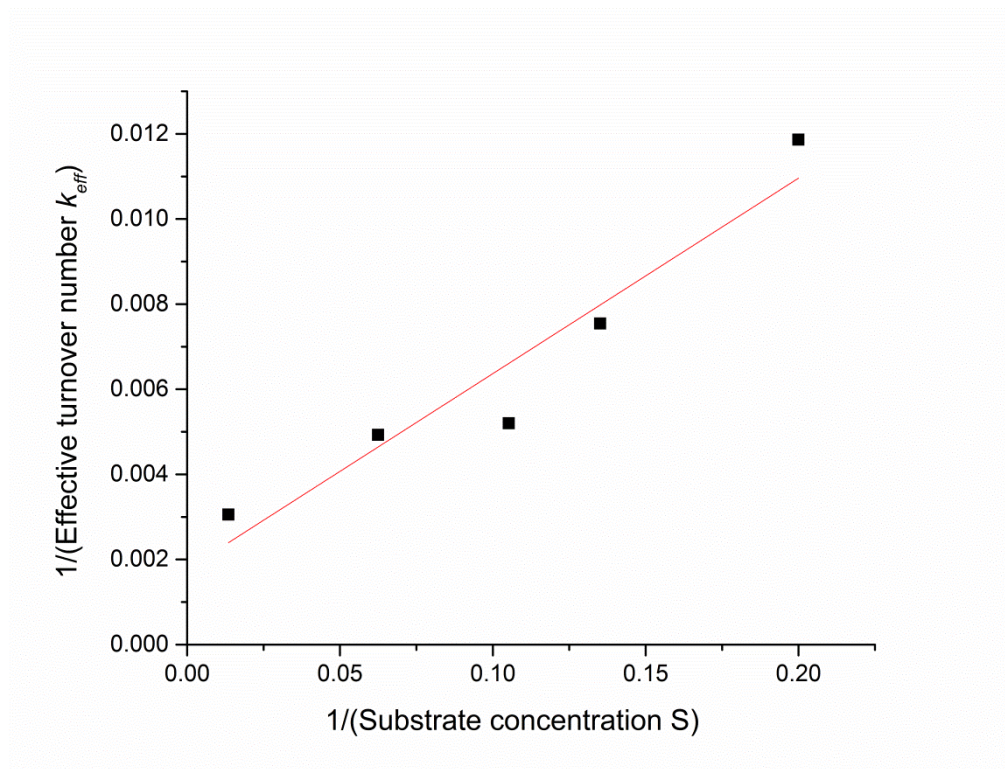


Figure 4 Catalytic kinetics of single soft nanoparticles: reciprocal of effective turnover number estimated according to Equation 1 versus reciprocal of TCE substrates (black dots), Linear fitting (red line) to the experimental data given by Equation 4.

The linear relation between $\frac{1}{k_{eff}}$ and $\frac{1}{[TCE]}$ is consistent with the proposed mechanism above for catalytic efficiency of dehalogenation by single soft nanoparticles. Further from the linear fitting by Equation 4 with the experimental data (Figure 4), the kinetic constant K and the maximum turnover number k_{cat} for single soft nanoparticle can be estimated as 26 ± 4 mM and 565 ± 290 s⁻¹, respectively. Then, the catalytic efficiency of single soft nanoparticles k_{cat}/K is estimated to be 2.2×10^4 M⁻¹s⁻¹. The maximum turn-over number is found significantly higher than the dehalogenation reported on B₁₂ molecules covalently immobilised onto the electrode where in the latter case a multi-layer film was likely formed [6c].

To our knowledge, this is the first time that the kinetics and turnover frequency of single individual soft nanoparticles have been *quantitatively* measured and analysed. We believe this is a new strategy to fundamentally explore catalytic reaction of soft nanoparticles with the mechanistic simplification offered allowing insights into catalytic kinetics at single-individual-nanoparticle resolution, likely opening doors for discoveries and rational designs of soft nanoparticles and enzyme nanocarriers

which are currently neglected but hold promise as more affordable and natural non-metal catalysts for diverse chemical reactions and applications.

Reference

- [1] a) P. Chen, X. C. Zhou, N. M. Andoy, K. S. Han, E. Choudhary, N. M. Zou, G. Q. Chen, H. Shen, *Chem Soc Rev* **2014**, *43*, 1107-1117; b) X. N. Shan, I. Diez-Perez, L. J. Wang, P. Wiktor, Y. Gu, L. H. Zhang, W. Wang, J. Lu, S. P. Wang, Q. H. Gong, J. H. Li, N. J. Tao, *Nat Nanotechnol* **2012**, *7*, 668-672; c) W. L. Xu, J. S. Kong, Y. T. E. Yeh, P. Chen, *Nat Mater* **2008**, *7*, 992-996; d) Y. W. Zhang, J. M. Lucas, P. Song, B. Beberwyck, Q. Fu, W. L. Xu, A. P. Alivisatos, *P Natl Acad Sci USA* **2015**, *112*, 8959-8964.
- [2] a) S. E. Fosdick, M. J. Anderson, E. G. Nettleton, R. M. Crooks, *J Am Chem Soc* **2013**, *135*, 5994-5997; b) R. Dasari, D. A. Robinson, K. J. Stevenson, *J Am Chem Soc* **2013**, *135*, 570-573; c) A. J. Bard, H. J. Zhou, S. J. Kwon, *Isr J Chem* **2010**, *50*, 267-276; d) W. Cheng, R. G. Compton, *Trac-Trend Anal Chem* **2014**, *58*, 79-89; e) N. V. Rees, *Electrochemistry Communications* **2014**, *43*, 83-86. f) L. Wang, A. Ambrosi, M. Pumera, *Angew Chem Int Edit* **2013**, *52*, 13818-13821; g) M. Pumera, *Acs Nano* **2014**, *8*, 7555-7558; h) J. M. Kahk, N. V. Rees, J. Pillay, R. Tshikhudo, S. Vilakazi, R. G. Compton, *Nano Today* **2012**, *7*, 174-179; i) Y. G. Zhou, N. V. Rees, R. G. Compton, *Angew Chem Int Edit* **2011**, *50*, 4219-4221; j) E. J. E. Stuart, K. Tschulik, C. Batchelor-McAuley, R. G. Compton, *Acs Nano* **2014**, *8*, 7648-7654; k) X. F. Zhou, W. Cheng, R. G. Compton, *Angew Chem Int Edit* **2014**, *53*, 12587-12589. l) W. Cheng, X. F. Zhou, R. G. Compton, *Angew Chem Int Edit* **2013**, *52*, 12980-12982; m) X. Y. Xiao, A. J. Bard, *J Am Chem Soc* **2007**, *129*, 9610-9612; n) X. Y. Xiao, F. R. F. Fan, J. P. Zhou, A. J. Bard, *J Am Chem Soc* **2008**, *130*, 16669-16677.
- [3] a) W. Cheng, R. G. Compton, *Angew Chem Int Edit* **2014**, *53*, 13928-13930; b) J. Dunevall, H. Fathali, N. Najafinobar, J. Lovric, J. Wigstrom, A. S. Cans, A. G. Ewing, *J Am Chem Soc* **2015**, *137*, 4344-4346; c) J. E. Dick, A. T. Hilterbrand, A. Boika, J. W. Upton, A. J. Bard, *P Natl Acad Sci USA* **2015**, *112*, 5303-5308; d) H. S. Toh, R. G. Compton, *Chem Sci* **2015**, *6*, 5053-5058; e) W. Cheng, R. G. Compton, *Angew Chem Int Edit* **2015**, *54*, 7082-7085; f) B. K. Kim, J. Kim, A. J. Bard, *J Am Chem Soc* **2015**, *137*, 2343-2349; g) B. K. Kim, A. Boika, J. Kim, J. E. Dick, A. J. Bard, *J Am Chem Soc* **2014**, *136*, 4849-4852; h) J. E. Dick, C. Renault, B. K. Kim, A. J. Bard, *Angew Chem Int Edit* **2014**, *53*, 11859-11862; i) J. E. Dick, C. Renault, B. K. Kim, A. J. Bard, *J Am Chem Soc* **2014**, *136*, 13546-13549. j) J. E. Dick, C. Renault, A. J. Bard, *J Am Chem Soc* **2015**, *137*, 8376-8379. k) X. Li, S. Majdi, J. Dunevall, H. Fathali, A. G. Ewing, *Angew. Chem. Int. Ed.*, **2015**, *54*: 11978-11982. l) C. E. Banks, N. V. Rees, R. G. Compton, *J Electroanal Chem* **2002**, *535*, 41-47; m) C. E. Banks, N. V. Rees, R. G. Compton, *J Phys Chem B* **2002**, *106*, 5810-5813
- [4] a) S. Nayak, L. A. Lyon, *Angew Chem Int Edit* **2005**, *44*, 7686-7708; b) S. E. F. Kleijn, S. C. S. Lai, M. T. M. Koper, P. R. Unwin, *Angew Chem Int Edit* **2014**, *53*, 3558-3586. c) F. Zaera, *Chem Soc Rev* **2013**, *42*, 2746-2762;
- [5] a) F. Zelder, *Chem Commun* **2015**, *51*, 14004-14017. b) M. Giedyk, K. Goliszewskaab, D. Gryko, *Chem. Soc. Rev.*, **2015**, *44*, 3391-3404.
- [6] a) C. Costentin, M. Robert, J. M. Saveant, *J Am Chem Soc* **2005**, *127*, 12154-12155; b) S. T. Chang, C. H. Wang, H. Y. Du, H. C. Hsu, C. M. Kang, C. C. Chen, J. C. S. Wu, S. C. Yen, W. F. Huang, L. C. Chen, M. C. Lin, K. H. Chen, *Energ Environ Sci* **2012**, *5*, 5305-5314; c) H. Shimakoshi, M. Tokunaga, K. Kuroiwa, N. Kimizuka, Y. Hisaeda, *Chem Commun* **2004**, 50-51. d) T. F. Connors, J. V. Arena, J. F. Rusling, *J Phys Chem* **1988**, *92*, 2810-2816. e) D. Lexa, J. M. Saveant, *Accounts Chem Res* **1983**, *16*, 235-243. d) Y. H. Kim, E. R. Carraway, *Environ Technol* **2002**, *23*, 1135-1145.
- [7] K. A. P. Payne, C. P. Quezada, K. Fisher, M. S. Dunstan, F. A. Collins, H. Sjuts, C. Levy, S. Hay, S. E. J. Rigby, D. Leys, *Nature* **2015**, *517*, 513-516.

- [8] a) J. F. Rusling, T. F. Connors, A. Owlia, *Anal Chem* **1987**, 59, 2123-2127; b) P. Tomcik, C. E. Banks, T. J. Davies, R. G. Compton, *Anal Chem* **2004**, 76, 161-165.
- [9] a) C. E. Banks, T. J. Davies, R. G. Evans, G. Hignett, A. J. Wain, N. S. Lawrence, J. D. Wadhawan, F. Marken, R. G. Compton, *Phys Chem Chem Phys* **2003**, 5, 4053-4069. b) T. J. Davies, A. C. Garner, S. G. Davies, R. G. Compton, *J Electroanal Chem* **2004**, 570, 171-185.

Graphic Abstract

